Progress of Theoretical Physics, Vol. 106, No. 4, October 2001

Systematic Analysis of Periodic Vegetation Patterns

Tomoo Okayasu[1,*] and Yoji Aizawa[2]

[1]*Graduate School of Science and Engineering, Waseda University, Tokyo 169-8555 Japan*

[2]*School of Science and Engineering, Waseda University, Tokyo 169-8555, Japan*

(Received July 3, 2001)

Spatially periodic vegetation patterns are observed in many semiarid regions. They are classified according to their symmetry as vegetation stripes on hillsides or spotted patterns on flat ground. We propose a simple model based on the interactions among water, soil and vegetation, which gives a systematic description of the variety of vegetation patterns. First, it describes most characteristics of vegetation stripes investigated in field observations and agrees with the hypothesized origin of vegetation stripes deduced from field observations, the spatially heterogeneous infiltration rate of surface water into soil. Moreover, it indicates that spotted patterns emerge from the same dynamics. Second, the pattern selection derived from the model is consistent with that found in real phenomena, i.e. predominantly bare ground with spotted vegetation in the most severe environments, banded patterns in intermediate environments and nearly continuous vegetation with spotted bare ground in the most favorable environments.

§1. Introduction

In 1950, Macfadyen discovered a spatially periodic vegetation pattern in a semi-arid region of British Somaliland.[1)] A great deal of similar phenomena have been reported since then, observed in semi-arid regions of Africa, America and Australia.[2)] Spatially periodic vegetation patterns are classified as vegetation stripes (Fig. 1) and spotted bush (Fig. 2), according to their symmetry. Vegetation stripes, in which dense bands are separated by nearly bare ground, extend to tens of square kilometers. Their wavelength varies from tens to hundreds of meters. Vegetation consisting of spots separated by bare ground is called 'spotted bush'. There are few studies of spotted bush, because it has been considered random patches, due to its irregularity. By contrast, there are many studies of vegetation stripes. In these studies, the emergence and maintenance of vegetation stripes was thought to originate in the inherent nature of the semi-arid ecosystem.[3)-8)]

Many phenomena in which regularity is organized in an open system have been observed in various disciplines of natural sciences: physics, chemistry and biology.[9)] The framework of dissipative structures provide a theory to describe them, spatio-temporal periodic phenomena in particular.[10)] Lefever and Lejeune[11)] developed the first model of vegetation patterns on the basis of the framework of dissipative structures. Though their model is successful in providing an integrated description of vegetation stripes and spotted bush, it employs rather abstract terminology from

*) Present address: Graduate School of Agricultural and Life Science, The University of Tokyo, Tokyo 113-8657. E-mail: aa17005@mail.ecc.u-tokyo.ac.jp

the biological viewpoint. In this paper, we propose a model based on dissipative structures that gives a systematic description of vegetation patterns, with components that are clearly defined in biology.

Field observations

Most vegetation stripes form in regions categorized as semi-arid, where the mean annual rainfall is about 200mm,[4),5)] while some stripes exist in more arid regions (with annual rainfall from 50 mm to 100 mm)[12)] and sub-humid regions (400 mm to 700 mm).[3)] The period of such patterns is from tens to hundreds of meters. White[12)] reported that the width of the bands and lanes (bare ground) is 40m and 150m, respectively. Other surveys have found 20m and 50m,[3)] and 90 to 180m and 45m.[5)] The territory in which vegetation stripes are dominant extends to tens of square kilometers.[5),12)]

In general, rainfall occurs intermittently in arid regions. Sometimes the amount of rainfall in a day is more than the mean annual rainfall, and rainfall is always too intense to infiltrate into soil immediately. Thus in general, "sheet wash" sweeps the entire region. Sheet wash is observed in regions where vegetation stripes exist.[13),6),12),4)] Sheet wash is defined as water flow that covers the surface of a vast region and does not run inside particular lanes.

Vegetation stripes are observed in various regions. Most of them are in parts of Africa, such as Niger,[3)] Burkina Faso,[14)] Somalia,[1),5),7)] and Ethiopia,[5)] as well as in Mexico.[4)] Stripes have also been reported to form on various types of soil: silt,[12),13)] mud,[12)] gravel,[3)] clay,[15)] sand[13)] and crust.[5)] Therefore, the origin of vegetation stripes apparently does not depend on the soil type. Moreover, specific

Fig. 1. Example of vegetation stripes in Somaliland.[13)] The black regions represent vegetation, and the white regions represent bare ground.

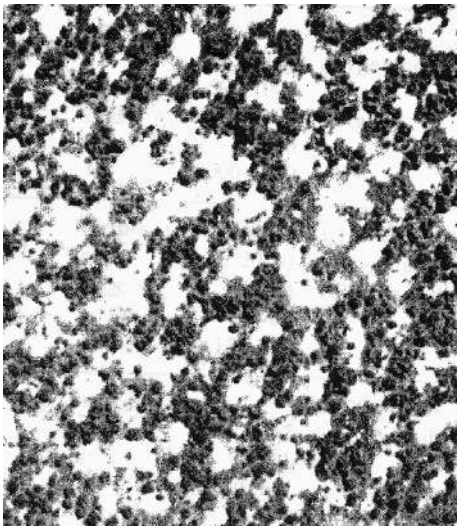

Fig. 2. Example of spotted bush in north west Burkina Faso.[17)] The black regions represent vegetation, and the white regions represent bare ground.

plant species are not necessary to form vegetation stripes. Thus stripes formation seems to be a universal phenomenon in semi-arid ecosystems.

Vegetation stripes have some interesting properties. First, the stripes are oriented parallel to the contour line.[4),6),12)] Second, stripes slowly move uphill.[4),6),7),16)] Third, the plants located on the upward side of a band thrive, while those on the downward side of a band tend to die out.[4)] The resulting upward migration provides evidence that the origin of vegetation stripes is an inherent phenomenon, because the autonomous migration of the external environment is much less realistic. The comparisons of the properties of vegetation patterns in various regions have been summarized by Lejeune et al.[18)]

As mentioned above, spotted bush has not been studied extensively, and it is usually recognized as random patches.[3),19)] However, Couteron et al.[14)] verified through Fourier analysis that patterns of "random patches" possess hexagonal periodicity.

Hypothesized origin of stripes from field observations

Field investigation suggests that the higher infiltration rate of surface water into soil in bands than in bare ground results in vegetation stripes.[3)-8)] In such a situation, rainfall infiltrates bare ground only very little, and runs away into downward bands, where most of the water is absorbed into the soil. Due to the shortage of water in the bare grounds, vegetation decreases, and as a result, the infiltration rate into bare ground becomes even smaller. Contrastingly, a positive feedback exists in bands. This circulation maintains the spatially heterogeneous infiltration rate. The dynamics of upward migration of bands and the heterogeneity of vegetation in a band support this hypothesis.

At positions several centimeters above the upside boundary of a band in bare ground, a great deal of germination phenomena are observed. This suggests that large amounts of water are available there. By contrast, in the downside of a band,

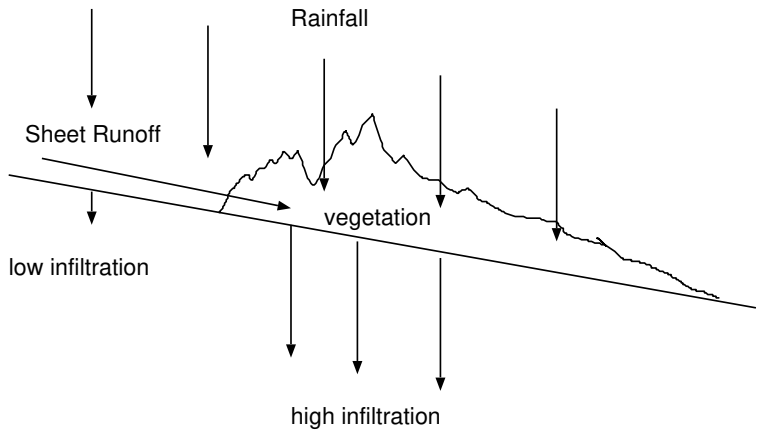

Fig. 3. A schematic representation of the mechanism by which the vegetation areas receive abundant water. Because of a low infiltration rate in bare areas, most of the water falling on these areas flows into vegetation areas, where much water infiltrates into the soil.

many plants die, because water is insufficient there. This results in the upward migration of bands. These dynamics are depicted in Fig. 3.

Model development for vegetation stripes

Mauchamp [20] carried out detailed numerical simulations that take such a positive feedback system into account. The results exhibit the spatial heterogeneity of vegetation. However, his one-dimensional model could not account for stripes (which are two dimensional) nor migration phenomena, because the location of the upside boundary of a band is fixed at the origin of the simulation space.

The first quantitative analysis of the formation of stripes based on a heterogeneous infiltration rate was proposed by Klausmeier. [21] That model consists of a two-dimensional coupled partial differential equations describing water and biomass. Stripes and their upward migration were observed in numerical simulations, while no spatial patterns appeared in the spatially isotropic case. He concluded that microrelief is the cause of irregular patterns, which correspond to random patches in real phenomena.

Lefever's mean-field propagator-inhibitor model

To this time, no study has been successful in showing intrinsic patterns without exogenous spatial heterogeneity, except Lefever's mean-field propagator-inhibitor model. [11] That model yields spatial patterns caused by an intrinsic mechanism without exogenous spatial anisotropy. He claimed that the hexagonal pattern in the isotropic case corresponds to the pattern on flat ground in a real field. His model may be capable of providing an integrated description of vegetation stripes and spotted bush with the same origin.

Though his research is significant from the viewpoint of integration, pattern formation in his model requires that the ratio of the area of cooperative interaction to that of competitive interaction be much smaller than 1. This condition has no relation to the origin hypothesized by field researchers nor the positive feedback structure. Moreover, the concept of cooperation and competition is too abstract to compare with the real phenomena.

§2. Model

The model we use to describe such systems should consist of only measurable components, such as water, soil, plants and their interactions, to facilitate comparison with field observations. In addition, the spatial scales of vegetation patterns are much greater than those of individual plants. For this reason, partial differential equations are adopted.

Water balance and transport

Transport of water plays an essential role in determining the large-scale structure of vegetation patterns, whose dynamical mechanisms have been studied by Klausmeier [21] and Mauchamp [20] in detail. However, their studies have been limited only to the formation of vegetation stripes. In our opinion, a variety of vegetation

patterns should be systematically explained from the unified viewpoint of dynamical modeling, taking the role of water transport into account.

In our investigations, the water content of the ground surface and in the soil are treated separately, and the balance equations are given by

$$\frac{\partial w(\vec{r},t)}{\partial t} = P - E - I + F + D_w, \tag{2·1}$$

$$\frac{\partial s(\vec{r},t)}{\partial t} = I - U + D_s, \tag{2·2}$$

where w represents the amount of water on the ground surface, s the amount of water in the soil, P the water input, E the evaporation, I the surface water infiltration into soil, F the surface water flow, D_w the surface water diffusion, U the root water uptake, and D_s the soil water diffusion.

For each factor, we adopt the simplest form that does not qualitatively contradict field observations. Rainfall is assumed to occur constantly, i.e. $P = a$, where a represents rainfall amount [kg/year]. Evaporation is assumed to be proportional to the amount of surface water $w(\vec{r},t)$, i.e. $E = lw(\vec{r},t)$, where l is the evaporation rate [year^{-1}]. As plants grow, soil is formed through the deposition of dead plant matter. Thus, surface water infiltration increases as biomass increases. Naturally, since the field capacity is not infinite, the amount of soil water has an upper limit, which increases as the biomass increases.

We assume that the field capacity is proportional to the biomass, because the long term accumulation of deposited plant matter can be ignored, due to intensive sheet wash. Therefore, the field capacity is assumed to take the form $n(\vec{r},t)f$ here, where $n(\vec{r},t)$ is the biomass and f is field capacity per unit biomass. Thus, infiltration can be written

$$I = kn(\vec{r},t)w(\vec{r},t)\left(1 - \frac{s(\vec{r},t)}{n(\vec{r},t)f}\right),$$

where k is the infiltration rate.

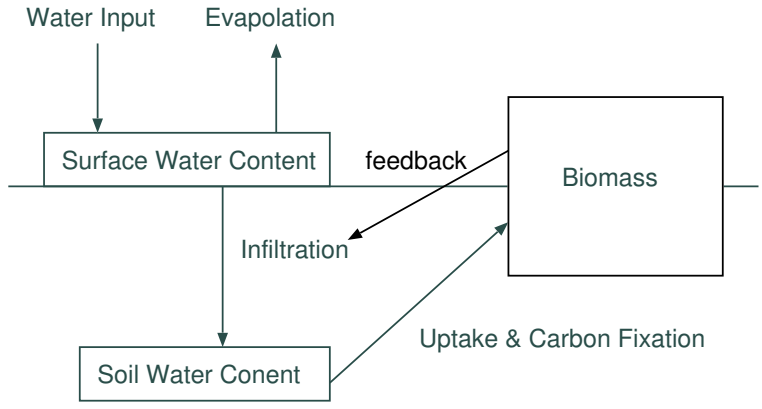

Fig. 4. The feedback mechanism between water infiltration and biomass.

Plants absorb water stored in soil, and the amount of absorbed water increases as the biomass increases and the amount of water increases. Thus we have $U = pn(\vec{r},t)s(\vec{r},t)$, where p is the water intake rate.

When surface water exists on sloping ground, water flows downward. The direction of maximal slope is taken to be x, without loss of generality, so it can be expressed as $F = A_r \frac{\partial w(\vec{r},t)}{\partial x}$, where A_r is the slope constant. Even if the field is flat, water naturally tends to diffuse. This implies $D_w = D_w \nabla^2 w(\vec{r},t)$ and $D_s = D_s \nabla^2 s(\vec{r},t)$, where D_w is the diffusion rate of surface water and D_s that for soil water.

Plant growth and reproduction

We assume that the amount of water is the only limiting factor. Thus the equation for biomass in this model should not contain saturation term. The simplest growth model consists of the following well-known equation (for example, see Ref. 22)):

$$\frac{\partial n(\vec{r},t)}{\partial t} = G - M + D_n \nabla^2 n(\vec{r},t). \tag{2·3}$$

Here n is the biomass [kg], G the plant growth [kg/year], and M the mortality [kg/year]. As expressed in this equation, plant propagation is represented as diffusion with diffusion rate D_n. Competition for water is contained here in the growth term G. Because the amount of carbon fixation is proportional to that of root water uptake, $pn(\vec{r},t)s(\vec{r},t)$, it is simply expressed as $qpn(\vec{r},t)s(\vec{r},t)$. Plant mortality is assumed to have a constant rate m with $M = mn(\vec{r},t)$. The structure of the model is summarized in Fig. 4.

§3. Uniform steady state distribution

For simplicity, we use dimensionless quantities, defined as

$$\begin{aligned}
\{x', y', t'\} &= \left\{ \sqrt{\frac{l}{D_n}} x, \sqrt{\frac{l}{D_n}} y, lt \right\}, \\
\{w', s', n'\} &= \left\{ \frac{l}{a} w, \frac{l}{a} s, \frac{k}{l} n \right\}, \\
\{D_1, D_2, A_r'\} &= \left\{ \frac{D_w}{D_n}, \frac{D_s}{D_n}, (lD_n)^{-\frac{1}{2}} A_r \right\}, \\
\{f', p', q', m'\} &= \left\{ \frac{l^2}{ak} f, \frac{p}{k}, \frac{qka}{l^2}, \frac{m}{l} \right\}.
\end{aligned}$$

Omitting the primes on the dimensionless quantities, the whole model is given by

$$\begin{aligned}
\frac{\partial w(\vec{r},t)}{\partial t} &= 1 - w(\vec{r},t) - n(\vec{r},t) w(\vec{r},t) \left(1 - \frac{s(\vec{r},t)}{n(\vec{r},t) f} \right) + A_r \frac{\partial w(\vec{r},t)}{\partial x} + D_1 \nabla^2 w(\vec{r},t), \\
\frac{\partial s(\vec{r},t)}{\partial t} &= n(\vec{r},t) w(\vec{r},t) \left(1 - \frac{s(\vec{r},t)}{n(\vec{r},t) f} \right) - pn(\vec{r},t) s(\vec{r},t) + D_2 \nabla^2 s(\vec{r},t),
\end{aligned}$$

$$\frac{\partial n(\vec{r},t)}{\partial t} = qpn(\vec{r},t)s(\vec{r},t) - mn(\vec{r},t) + \nabla^2 n(\vec{r},t), \tag{3·1}$$

where the exogenous parameters are f, p, q, m, A_r, D_1 and D_2.

First, spatially homogeneous solutions are given. With these, all terms that include spatial differentiation disappear. In this case, it is easy to solve the equation, and we find three branches:

$$\begin{cases} w_0 = 1, \\ s_0 = 0, \\ n_0 = 0, \end{cases}$$
$$\begin{cases} w_{1\pm} = -\frac{1}{2fpq^2}(m^2 - fmpq - fpq^2 \pm \sqrt{-4fm^2pq^2 + (m^2 - fmpq + fpq^2)^2}), \\ s_1 = \frac{m}{pq}, \\ n_{1\mp} = -\frac{1}{2fmpq}(-m^2 + fmpq - fpq^2 \mp \sqrt{-4fm^2pq^2 + (m^2 - fmpq + fpq^2)^2}). \end{cases} \tag{3·2}$$

The first branch, w_0, s_0, n_0, represents the situation in which there is no vegetation. As found by linear stability analysis, this branch is stable in the entire parameter space. The second branch, w_{1+}, s_1, n_{1-}, corresponds to the situation in which vegetation exists. Negative values of this branch are not realized in the case that the initial values of w, s and n are positive. The third branch, w_{1-}, s_1, n_{1+}, can be ignored because it is unstable for any set of parameter values. Positive and stable sets of w, s and n are depicted in Fig. 5.

There exists a stability condition for the second branch,

$$-4fm^2pq^2 + (m^2 - fmpq + fpq^2)^2 > 0. \tag{3·3}$$

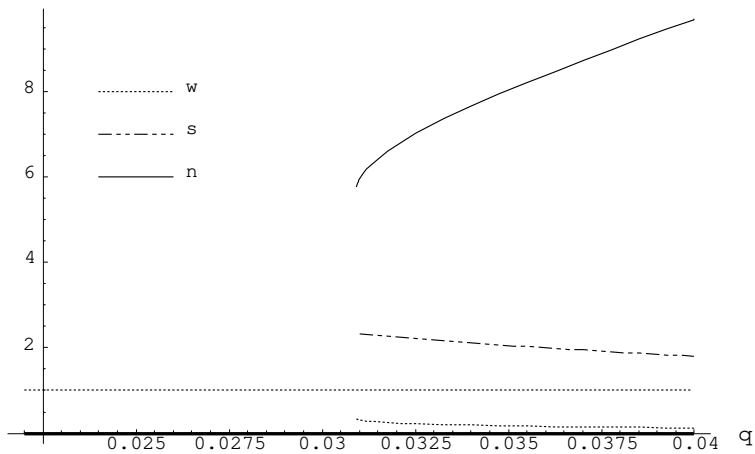

Fig. 5. Positive and stable uniform steady state solutions of the model ($f = 0.625$, $p = 0.05$, $m = 0.0036$).

Solving this for q, we find the bifurcation point shown in Fig. 5,

$$q_{+c} = \frac{m}{2}\left(1 + \frac{2}{\sqrt{fp}} + \frac{\sqrt{4+\sqrt{fp}}}{(fp)^{1/4}}\right). \tag{3·4}$$

An increase of q corresponds to a more favorable external environment for plant growth. More precipitation is a typical example. From this point of view, when the environment is too severe, vegetation cannot exist. Then, above some threshold value of q, plants can grow. It is interesting that the no vegetation branch is stable even when parameter values are above this threshold. In a real field, even if there existed stable vegetation in the past, it can be lost through soil degradation, in which case it is difficult to recover. Such a situation can be interpreted as corresponding to the no vegetation branch.

§4. Linear stability analysis

In the previous section, spatially homogeneous solutions were discussed. In this section, we investigate the characteristics of spatial patterns, because the model can exhibit Turing-like patterns (which appear due to the instability of a particular positive wavenumber when the set of parameters is beyond a specific threshold,[23] as shown below).

First, the dispersion relation of the no-vegetation branch, w_0, s_0, n_0, is found:

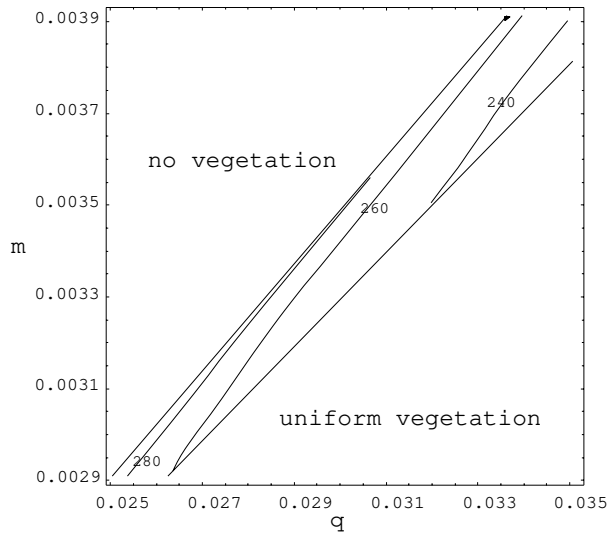

Fig. 6. Behavior of the model as determined by the paramaters q and m for $f = 0.625$, $p = 0.05$, $q = 0.0326$, $m = 0.0036$, $D_1 = 10000$, $D_2 = 10$ and $A_r = 0$. The contours represent the dimensional stripe wavelength as determined by the most unstable mode found through a linear stability analysis.

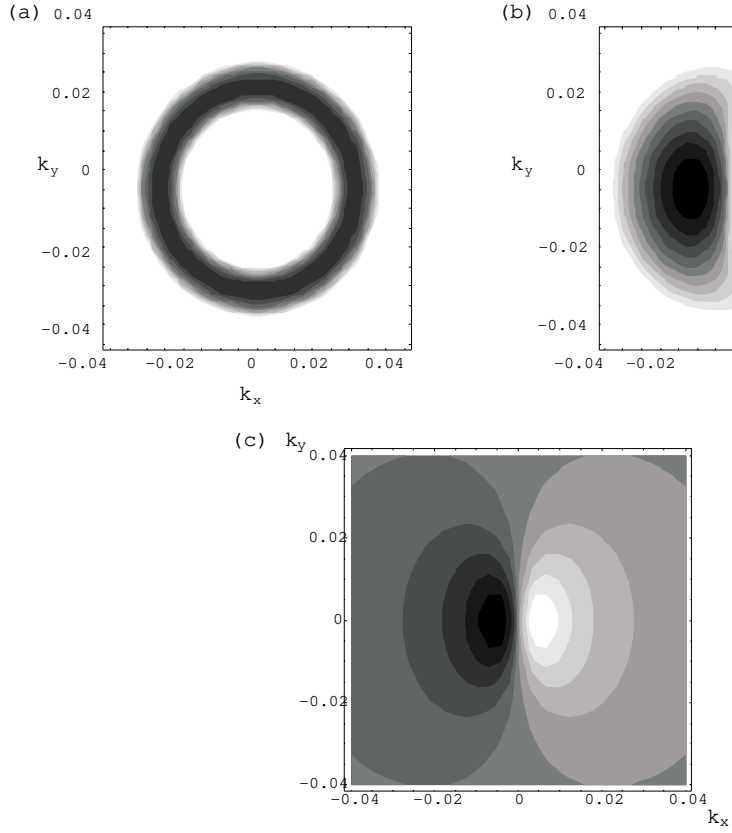

Fig. 7. The behavior of the real part of $\omega_{\vec{k}}$ in (a) the isotropic case ($A_r = 0$) and (b) the anisotropic case ($A_r = 500$). The other parameters are the same ($f = 0.625$, $p = 0.05$, $q = 0.0326$, $m = 0.0036$, $D_1 = 10000$, $D_2 = 10$). In (c), the behavior of the imaginary part of $\omega_{\vec{k}}$ with the same parameters as in (b) is shown. The white regions in the figures correspond to the domain in which the maximum eigenvalue is negative. The maximum eigenvalue for (a) is around 1.15×10^{-4}, while that for (b) is around 1×10^{-3}.

$$\begin{cases} \omega_0 = -1 + iA_r kx - D_1|k|^2, \\ \omega_1 = -\frac{1}{2}(1 + D_2|k|^2), \\ \omega_2 = -|k|^2 - m. \end{cases} \tag{4·1}$$

All of these eigenvalues are negative for any set of parameter values. Thus the only solution is spatially homogeneous. Then, the dispersion relation of the second branch is a root of

$$\begin{vmatrix} -w_1 A & \frac{s_1 w_1}{f} & -n_1 w_1 \\ \left(n_1 - \frac{s_1}{f}\right) & -\frac{s_1}{f}(D_2 f k^2 + w_1) + \omega + p n_1 & n_1(w_1 - p s_1) \\ 0 & pq n_1 s_1 & -n_1 B \end{vmatrix} = 0, \tag{4·2}$$

where $A = (1 + D_1 k^2 + n_1 + \omega - ik_x A_r)f - \frac{s_1}{f}$ and $B = k^2 + m - pqs_1 + \omega$.

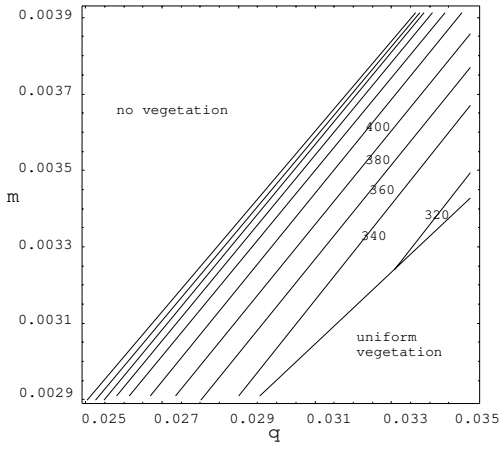

Fig. 8. The behavior of the model as determined by the parameters q and m in the anisotropic case ($f = 0.625$, $p = 0.05$, $q = 0.0326$, $m = 0.0036$, $D_1 = 10000$, $D_2 = 10$, A_r=500). The contours represent the dimensional stripe wavelengths in meters, as determined by the most unstable mode, found by the linear stability analysis.

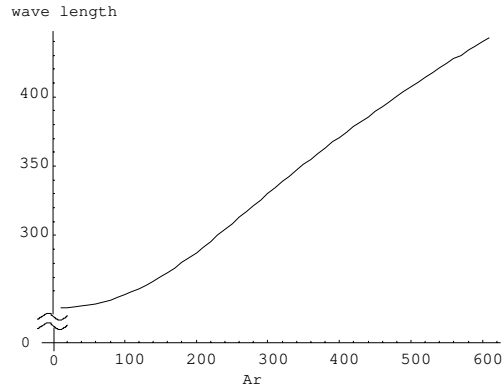

Fig. 9. The behavior of the wavelength for the maximum eigenvalue as a function of A_r ($f = 0.625$, $p = 0.05$, $q = 0.032$, $m = 0.0036$, $D_1 = 10000$, $D_2 = 10$).

The explicit forms of the eigenvalues are too complicated to be written here, because the eigenvalues are the roots of a third degree equation. First, we investigate the isotropic case ($A_r = 0$). Here, two of the three eigenvalues always have negative values. The other, $\omega_0(k)$, can have a positive value, or it can be unstable inside a particular range of parameter values. The quantity $\omega_0(k)$ satisfies the condition that it has a negative value at $k = 0$ and for $k \to \infty$. Thus, there can exist stable spatially periodic patterns. There exist marginal points, at which both $\omega_0(k_c) = 0$ and $\left.\frac{\partial\omega_0(k)}{\partial k}\right|_{k=k_c} = 0$ are satisfied, and the critical wavenumber k_c becomes unstable. There also exists a parameter range within which the eigenvalues of a finite range of wavenumbers between k_1 and k_2 have positive values. In the case that multiple wavenumbers become unstable simultaneously, the wavenumber that has the maximum eigenvalue is realized globally.[22] Therefore we investigate such a wavenumber to estimate the periodicity of realized spatial patterns (Fig. 6). As shown in the figure, the wavenumber of the spatial pattern becomes smaller as the external environment becomes more favorable. This result is consistent with field observations.

Next, we investigate the case in which exogenous anisotropy exists ($A_r \neq 0$). The maximum real parts of the eigenvalues for both the isotropic case and the anisotropic case are shown in Figs. 7(a) and (b). In the isotropic case, the unstable wavevectors are symmetric with respect to the origin, while the maxima are located at $(k_{\pm 0}, 0)$ in the anisotropic case. Therefore, the direction of the wavevector is parallel to the x axis. As shown in Fig. 7(c), in which the imaginary part of the wavenumber where

the eigenvalue has maximal real part is drawn, the imaginary part is non-zero where the real part is non-zero. This results in a typical Hopf bifurcation, followed by spatio-temporal periodicity.

The phase portrait of the maximum eigenvalue in the anisotropic case is shown in Fig. 8. In this case also, the wavenumber decreases as the external environment becomes favorable.

Finally, the slope dependence of the maximum eigenvalue on the slope constant is shown in Fig. 9 and compared with field observations, where the wavenumber decreases as the slope increases.

§5. Numerical simulation

Isotropic case

We studied the model equation numerically inside a 2-dimensional square region with periodic boundary conditions. The initial values were $w = 1$, $s = 1$ and $n = 10$, with small amplitude random noise.

In the isotropic case, in the beginning, the solution immediately converges to the spatially homogeneous steady state with weak noise. In the case that the set of parameter values is inside the unstable range, a spatially periodic pattern gradually appears. Typical patterns realized are striped, π-hexagonal and 0-hexagonal (Fig. 10). The π-hexagonal pattern is similar to the spotted bush in Burkina Faso (Fig. 2).

Pattern selection depends on parameter values. When the parameters correspond to a favorable environment, a spatially homogeneous steady state is realized. This seems to correspond to vegetation in a humid region, though in a real field, it is disturbed to form random patches. As the environment becomes worse, a spatially periodic steady state appears. This corresponds to spatially heterogeneous vegetation in an arid ecosystem. When the environment becomes more severe than a particular threshold, no vegetation is allowed. The last case corresponds to a

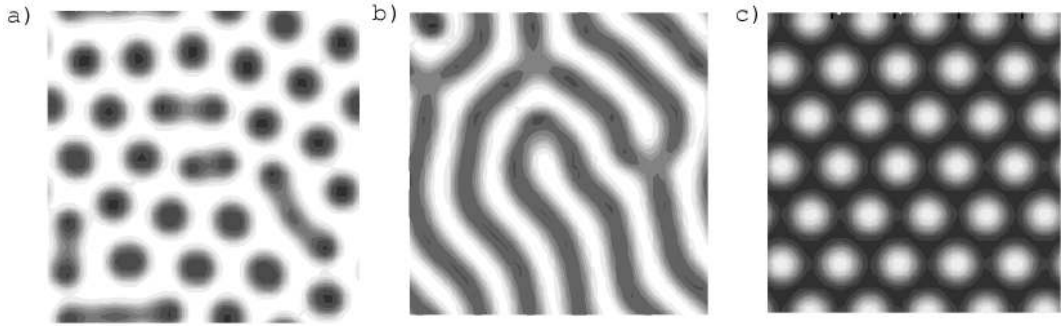

Fig. 10. Three examples of spatial patterns obtained for the isotropic case. Darker colors indicate higher vegetation densities: (a) 0-hexagonal ($f = 0.625$, $p = 0.05$, $q = 0.0798$, $m = 0.0096$, $D_1 = 10000$, $D_2 = 10$, $A_r = 0$); (b) stripe ($f = 0.625$, $p = 0.05$, $q = 0.09004$, $m = 0.0096$, $D_1 = 10000$, $D_2 = 10$, $A_r = 0$); and (c) π-hexagonal ($f = 0.625$, $p = 0.05$, $q = 0.09516$, $m = 0.0096$, $D_1 = 10000$, $D_2 = 10$, $A_r = 0$).

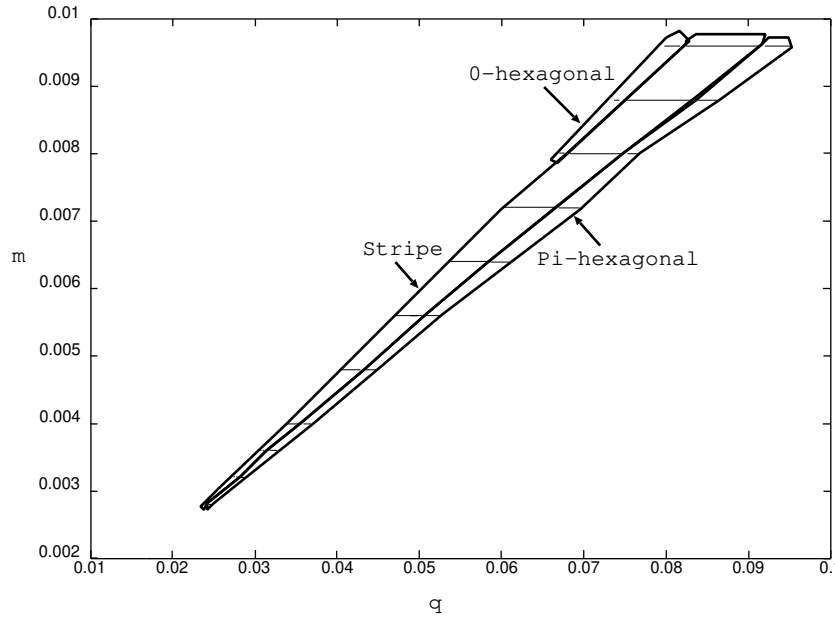

Fig. 11. Pattern selection obtained by numerical simulation for different sets of parameter values in the isotropic case ($f = 0.625$, $p = 0.05$, $D_1 = 10000$, $D_2 = 10$, $A_r = 0$). A 0-hexagonal pattern appears where the environment is severe, i.e., q is small and m is large. A striped pattern appears for intermediate environments, and a π-hexagonal pattern appears where the environment is relatively favorable.

hyper-arid region. Furthermore, the parameter values affect the pattern selection among the three periodic patterns. A π-hexagonal pattern is selected in a relatively favorable environment. By contrast, the parameter region for a 0-hexagonal pattern is located on the lower boundary with the no-vegetation region. Stripes form in an intermediate environment (Fig. 11).

Anisotropic case

When there is anisotropy, at first the solution converges to the homogeneous steady state immediately, and then, gradually, a one-dimensional striped pattern (Fig. 12) appears in the case that the parameters are in the unstable region. The wavevector of the stripes is directed along the x axis, and the stripes move toward the negative x direction (Fig. 13). Our numerical simulation results show that the final states are either spatially homogeneous or consist of such stripes. Thus we find that it is sufficient to treat the system as one dimensional. If we ignore the y direction, the equations become

$$\frac{\partial w(\vec{r},t)}{\partial t} = 1 - w(\vec{r},t) - n(\vec{r},t)w(\vec{r},t)\left(1 - \frac{s(\vec{r},t)}{n(\vec{r},t)f}\right) + A_r\frac{\partial w(\vec{r},t)}{\partial x} + D_1\frac{\partial^2 w(\vec{r},t)}{\partial x^2},$$

$$\frac{\partial s(\vec{r},t)}{\partial t} = n(\vec{r},t)w(\vec{r},t)\left(1 - \frac{s(\vec{r},t)}{n(\vec{r},t)f}\right) - pn(\vec{r},t)s(\vec{r},t) + D_2\frac{\partial^2 s(\vec{r},t)}{\partial x^2},$$

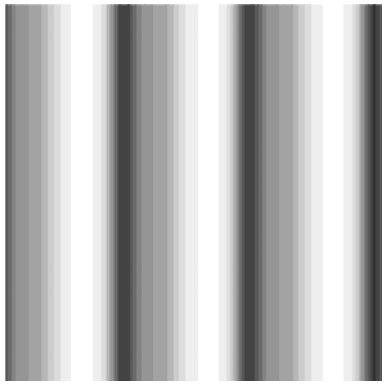

Fig. 12. Stripes moving in the direction from which water runs off for the anisotropic case ($f = 0.022727$, $p = 0.1$, $m = 0.036$, $q = 0.88$, $D_1 = 10000$, $D_2 = 10$, $A_r = 500$). Darker color indicates higher vegetation density.

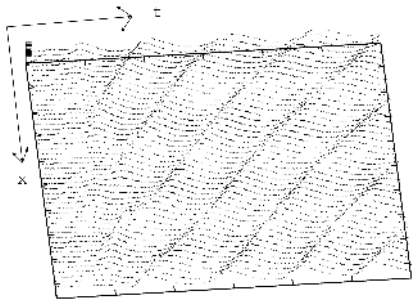

Fig. 13. Stripe movement in the negative x direction for the anisotropic case ($f = 0.625$, $p = 0.05$, $m = 0.0036$, $q = 0.032$, $D_1 = 10000$, $D_2 = 10$, $A_r = 300$).

$$\frac{\partial n(\vec{r},t)}{\partial t} = qpn(\vec{r},t)s(\vec{r},t) - mn(\vec{r},t) + \frac{\partial^2 n(\vec{r},t)}{\partial x^2}. \tag{5·1}$$

The direction $-x$ is opposite to the water flow. A large vegetation density is observed on the $-x$ side of a band, while a small vegetation density and gentle change of the vegetation density is observed on the lower side of a band in the solution. These characteristics agree with field observations.

§6. Discussion

In this paper, we have proposed a model that can systematically describe the dynamics of vegetation stripes and spotted bush, in which both patterns originate from the same structure, that is, a positive feedback mechanism among water, soil and plants.

Studies based on field investigations explain the reason that vegetation stripes are maintained as follows. In bare ground, water does not infiltrate and flows into downward bands due to a lack of soil. More water can accommodate more vegetation, and vice versa. Then, more vegetation provides more dead plant matter to form more soil. In such a system, the heterogeneity of soil water is maintained, and it directly affects that of vegetation. It can be determined whether such dynamics appear in the model from a snapshot of the amount of surface water, the amount of soil water and the vegetation density (Fig. 14). Where plants are prosperous, the amount of soil water is large. Contrastingly, the amount of surface water there is small. This state corresponds to the situation just after precipitation in the real world. Spatial patterns of the amount of infiltration are shown in Fig. 15. Clearly, large infiltration occurs where vegetation is dense. We thus see that the heterogeneity of the infiltration rate agrees with field observations. From the above findings, we conclude the following. (1) In the anisotropic case, the origin of vegetation stripes,

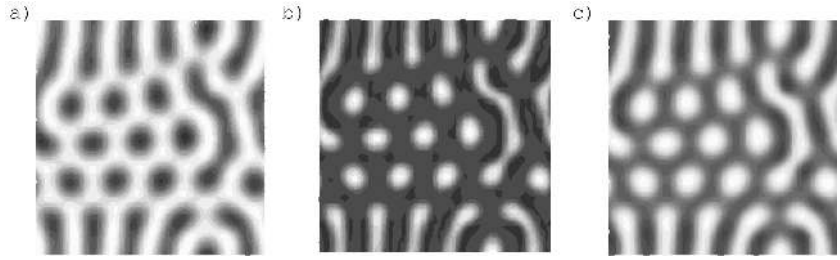

Fig. 14. Spatial patterns of (a) surface water, (b) soil water and (c) vegetation with $f = 0.625$, $p = 0.05$, $q = 0.10804$, $m = 0.0112$, $D_1 = 10000$, $D_2 = 10$ and $A_r = 300$. Darker colors indicate higher vegetation densities.

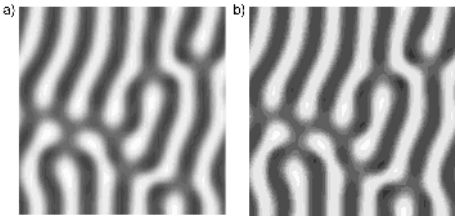

Fig. 15. Spatial patterns of (a) vegetation and (b) the amount of infiltration. Darker colors indicate higher vegetation densities.

or the heterogeneity of the infiltration rate agrees with that in the real world. (2) In the isotropic case, no field observations are available for hypothesizing its origin. However, the model indicates that it has the same origin as vegetation stripes.

Next, we discuss pattern selection behavior in the model. Couteron[14] carried out a diachronic comparison at a particular site between 1955, when the climate conditions were relatively humid, and 1984, after a severe drought. He pointed out that the pattern in 1955 was more or less spotted, and it was transformed into a banded pattern in 1984. This result can be interpreted as implying that a stripe pattern is formed when it is drier than the conditions for which a π-spotted pattern appears. Aguiar[24] indicated that the deteoriration of the external environment might cause the shift of patterns from striped to "leopard vegetation", which is similar to the 0-hexagonal pattern. These two results suggest that the pattern selected in the worst conditions is the 0-hexagonal pattern, the stripe pattern is formed in the intermediate situation, and the π-hexagonal pattern forms in good climate. The results of our model agree with these observations (see Fig. 11).

The result of our numerical simulations agrees with field observations in various respects: (a) stripes form where the external environment is relatively severe; (b) the direction of stripes is parallel to the contour lines; (c) the wavenumber of periodic patterns decreases as the external environment becomes worse; (d) the stripes migrate upward in the anisotropic case; (e) there is a large vegetation density on the upper side of a band, while there is a small vegetation density and gentle ecotone on the lower side.

Prospects

In this paper, the origin of vegetation patterns that we considered was restricted to the nature of the water in the system, for the purpose of simplification. Real phenomena are more complex and naturally contain many other factors, for example, wind and the behavior of animals.[24] Their effects should also be considered comprehensively. In addition, we assumed the further simplification of constant precipitation, though in arid regions, rainfall actually occurs intermittently. Because of such a simplification, several parameters, the evaporation rate, infiltration rate and water transportation in particular, cannot be compared with the values observed in a real field. Inclusion of the effect of intermittent precipitation is essential for comparing the model behavior to real phenomena, although most of the models developed in the past do not take this into account. In addition, it would be interesting to consider more detailed patterns in a band, like the heterogeneous pattern discovered by Boaler et al.[5]

Acknowledgements

The authors wish to acknowledge the useful suggestions and support of Professor Rene Lefever.

References

1) W. A. Macfadyen, Nature **165** (1950a), 121.
2) L. P. White, J. Ecol. **59** (1971), 615.
3) L. P. White, J. Ecol. **58** (1970), 549.
4) C. Montana, J. Lopez-Portillo and A. Mauchamp, J. Ecol. **78** (1990), 789.
5) S. B. Boaler and C. A. H. Hodge, J. Ecol. **50** (1962), 465.
6) S. B. Boaler and C. A. H. Hodge, J. Ecol. **52** (1964), 511.
7) C. F. Hemming, J. Ecol. **53** (1965), 57.
8) A. F. Cornet, J. P. Delhoume and C. Montana, in *Diversity and Pattern in Plant Communities*, ed. H. J. During, M. J. A. Werger and J. H. Willems (SPB Academic Publishing, Hague, 1988), p. 221.
9) H. Haken, *Synergetics : an introduction : nonequilibrium phase transitions and self-organization in physics, chemistry, and biology. Springer series in synergetics. Vol. 1.* (Springer-Verlag, Berlin, 1978).
10) G. Nicolis and I. Prigogine, *Self-organization in nonequilibrium systems : from dissipative structures to order through fluctuations* (Wiley, New York, 1977), p. 491.
11) R. Lefever and O. Lejeune, Bull. Math. Biol. **59(2)** (1997), 263.
12) L. P. White, J. Ecol. **57** (1969), 461.
13) W. A. Macfadyen, Geogr. J. **116** (1950b), 199.
14) P. Couteron, "Relation spatiales entre individus et structure d'ensemble dans des peuplements ligneux soudano-saheliens au nord-ouest du Burkina-Faso", Ph. D. thesis, University of Toulouse, France, 1998.
15) G. A. Worall, J. Soil Sci. **10** (1959), 34.
16) J. M. Thiery, J. M. d'Herbes and C. Valetin, J. Ecol. **83** (1995), 497.
17) R. Lefever, O. Lejeune and P. Couteron, in *Proceedings of the Workshop on Pattern Formation and Morphogenesis : Model Systems*, University of Minesota, Minneapolis, September 14-18, 1998.
18) O. Lejeune, P. Couteron and R. Lefever, Acta Oecol. **20(3)** (1999), 171.
19) A. J. Belsky, Ecology **75** (1994), 922.
20) A. Mauchamp, S. Rambal and J. Lepart, Ecol. Model. **71** (1994), 107.
21) C. A. Klausmeier, Science **284** (1999), 1826.

22) J. D. Murray, *Mathematical Biology. Biomathematics Texts. Vol. 19* (Springer-Verlag, Berlin/New York, 1989).
23) A. M. Turing, Phil. Trans. Roy. Soc. Lond., Ser. b **237** (1952), 37.
24) M. R. Aguiar and O. E. Sala, Tree **14-7** (1999), 273.